35th Annual International Conference of the IEEE EMBS
Osaka, Japan, 3 - 7 July, 2013

# Sensitivity of MRI for Directly Detecting Neuronal Electrical Activities in Rat Brain Slices

Dongmin Kim, Takao Someya, and Masaki Sekino, *Member, IEEE*

***Abstract*—We developed an experimental setup for magnetic resonance imaging (MRI) of rat brain slices maintained in a hemoglobin-free medium and showed that the MRI system has a sensitivity to magnetic fields of $10^{-11}$ T. The originally developed non-magnetic sample holder consisted of a microelectrode array for recording neuronal potentials and perfusing channels for the medium. Because of the hemoglobin-free condition, the magnetic fields could be distinguished from the baseline signal fluctuations due to hemoglobin. A theoretical estimation of the signal-to-noise ratio showed a sensitivity of $3.3 \times 10^{-10}$ T. Parameter optimization using a 7-T MRI system with the developed sample holder resulted in an experimental sensitivity of $4.0 \times 10^{-10}$ T. These MRI sensitivities potentially enable us to detect weak magnetic fields arising from neuronal activities, and are sufficiently high for detecting neuronal magnetic fields of $1.4 \times 10^{-11}$ T generated in rat brain slices by averaging signals 810 times.**

## I. Introduction

Conventional functional magnetic resonance imaging (fMRI) of brain activity is based mainly on signal variations caused by hemodynamic response through neurovascular coupling in the brain. This indirect measuring principle of conventional fMRI limits temporal resolution because of the delay in hemodynamic response of approximately 1 s following the occurrence of neuronal electric activities [1-2].

Direct detection of neuronal electric activities is expected to significantly improve the temporal resolution of fMRI from seconds to milliseconds. Feasibility of the direct MRI detection of neuronal activities has been evaluated in previous studies on phantoms, living animals, and humans [3-11]. The magnetic fields arising from the ionic currents associated with postsynaptic potentials are extremely weak. Bodurka et al. measured a very weak magnetic field of 200 pT generated from flowing current in a phantom [4]. However, in living animals, blood hemoglobin causes a considerable fluctuation of the local field distributions and makes it further difficult to detect the neuronal magnetic fields directly [12].

Employing hemoglobin-free sample enables us to eliminate the hemodynamic effects. In previous studies, direct detection has been attempted using cell cultures and snail ganglia maintained in a hemoglobin-free medium [13-14]. These samples provide feasible models of isolated neuronal cells. Meanwhile these results remain to be validated in terms of whether the sensitivity of MRI is sufficiently high to detect these neuronal activities or not.

In the present study, we developed an experimental setup of rat brain slices maintained in a hemoglobin-free medium for MRI and presented that the MRI system has sensitivity to weak magnetic fields of $10^{-11}$ T arising from neuronal activities. An MRI-compatible electrode chamber for maintaining an isolated rat brain slice in a hemoglobin-free medium of artificial cerebrospinal fluid (aCSF) was developed. In order to discuss the feasibility of detecting neuronal electric activities using MRI, we evaluated the sensitivity theoretically and experimentally based on the signal-to-noise ratio (SNR) in our measuring setup. The results indicated that the magnetic field intensity arising in the rat brain slice is higher than the sensitivity of MRI.

## II. Theoretical Sensitivity of MRI

The theoretical limit of sensitivity was analyzed based on the theory of the SNR in MRI [15]. Hatada et al. estimated the limit of sensitivity for detecting a weak magnetic field theoretically and experimentally in a phantom, and they also investigated the limit of sensitivity based on a finite element method (FEM)-based calculation in the human brain [8-9]. The calculation condition was substantially considered under the actual hemoglobin-free condition.

### A. Signal intensity

The magnetization $M_0$ induced in a sample by the main static magnetic field $B_0$ is given by

$$M_0 = \frac{N_s \gamma^2 \hbar^2 I(I+1) B_0}{3 k_B T_s} \qquad (1)$$

where $N_S$ is the $^1$H density of the sample, $\gamma$ is the gyromagnetic ratio of $^1$H ($\gamma = 2.67 \times 10^8$ rad/T·s), Planck's constant $\hbar = 1.05 \times 10^{-34}$ J, the spin quantum number $I = 1/2$, the Boltzmann constant $k_B = 1.38 \times 10^{-23}$ J/K, and $T_S$ is the absolute temperature of the sample. Moreover, the signal intensity $S$ per voxel in an MR image with a field of view (FOV) of $L \times L$ and a slice thickness of $h$ is given by

$$S = \gamma B_0 B_1 M_0 L^2 h \times \frac{\{1 - \exp(-T_R/T_1)\}\exp(-T_E/T_2^*)}{1 - \cos\theta \exp(-T_R/T_1)} \sin\theta \qquad (2)$$

where $T_R$ is the repetition time, $T_1$ and $T_2^*$ are the relaxation times of the sample, and $\theta$ is the flip angle. $B_1$ is the RF flux density of the magnetic field produced in a voxel by a unit current flowing in the detecting coil.

D. Kim, T. Someya, and M. Sekino are with the Department of Electrical Engineering and Information Systems, Graduate School of Engineering, University of Tokyo, Tokyo 1138656, Japan, and also with the Exploratory Research for Advanced Technology (ERATO), Japan Science and Technology Agency (JST), Tokyo 1130032, Japan. (e-mail: dongmin@bee.t.u-tokyo.ac.jp; someya@ee.t.u-tokyo.ac.jp; sekino@bee.t.u-tokyo.ac.jp)

*B. Noise*

In MR images, considerable noise sources are attributable to conductors in the detector coil and the sample. To calculate the noise in the detector coil and the sample, their effective resistances must be estimated.

The effective resistance $R_c$ of a one-turn coil is given by

$$R_C = \frac{l}{p}\sqrt{\frac{\mu_r \mu_0 \omega_0 \rho}{2}} \tag{3}$$

where $\rho$ is the resistivity of the coil conductor, $l$ is the length of the conductor, $p$ is the circumference, $\mu_r\mu_0$ is the permeability, and $\delta$ is the skin depth at radio frequency. The effective resistance $Rs$ in a columnar sample is given by

$$R_s = \frac{1}{8}\pi\sigma\omega_0^2 B_1^2 r_S^4 h \tag{4}$$

where the magnetic resonance frequency $\omega_o = \gamma B_0$, $\sigma$ is the conductivity of the sample, $r_s$ is the radius of the columnar sample, and $h$ is the height of the sample.

The Johnson noise $N$ per voxel in an MR image has $n \times n$ voxels because of the detector coil and the sample, and is given by

$$N = n\sqrt{4k_B \Delta f \left(T_C R_C + T_S R_S\right)} \tag{5}$$

where $\Delta f$ is the spectral width of the receiver circuit, $T_C$ is the absolute temperature of the detector coil, and $T_S$ is the absolute temperature of the sample.

*C. Theoretical limit of sensitivity*

The intensity $\beta$ of a weak magnetic field in a sample is estimated from a change in the MR signal. The uncertainty $\sigma_B$ in the estimated value of the magnetic field due to the noise in the MR signal is given by

$$\sigma_B = \frac{N}{S}\frac{1}{\gamma T_E \sqrt{n_{ave}}} \tag{6}$$

where $N$ and $S$ are the noise and signal intensity in the MR signal, respectively. Moreover, $T_E$ is the echo time, and $n_{ave}$ is the number of data in the averaging. For detecting weak magnetic fields, the MR signals are normally measured from a $^1$H nucleus because of high signal intensity. The weak magnetic field $\beta$ can be detected when $\beta$ is higher than the uncertainty $\sigma_B$. Thus, $\sigma_B$ gives the theoretical limit of sensitivity for the magnetic fields.

## III. Calculation Model

In order to evaluate the theoretical limit of sensitivity for detecting the neuronal electric activity directly in a rat brain slice, we assumed a calculation model as shown in Fig. 1. A rat brain slice with a thickness of 400 μm was merged with aCSF in a perfusion chamber with a diameter of 22 mm. The level of aCSF was stably maintained at 2 mm. A detecting coil with a diameter of 20 mm was placed 1.5 mm beneath the bottom of the perfusion chamber.

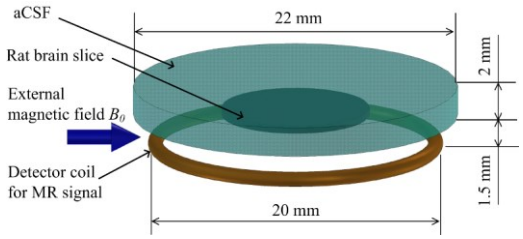


Figure 1. Analytical model of rat brain slice and MRI detector coil

In the calculation, the rat brain slice region was assumed as aCSF because the signal intensity of aCSF is stronger than that of the rat brain slice. The perfusion chamber was filled with aCSF homogeneously. Parameters such as the $T_1$ and $T_2$ relaxation times, conductivity, temperature, and density of $^1$H were used as listed in Table I. Table II lists the detailed parameters for the detecting coil.

TABLE I. ASSUMED PHYSICAL PARAMETERS OF RAT BRAIN SLICE

| | |
|---|---|
| $T_1$ relaxation time ($T_1$) | 1.9 s |
| $T_2$ relaxation time ($T_2$) | 0.25 s |
| Density of $^1$H ($N_s$) | $6.7 \times 10^{28}$ m$^{-3}$ |
| Conductivity ($\sigma$) | 2.2 S/m |
| Temperature of sample ($T_S$) | 308 K |

TABLE II. PARAMETERS OF DETECTING COIL

| | |
|---|---|
| Length ($l$) | $6.2 \times 10^{-2}$ m |
| Circumference ($p$) | $5.0 \times 10^{-3}$ m |
| Permeability ($\mu_r\mu_0$) | $1.26 \times 10^{-6}$ H·m$^{-1}$ |
| Radius ($r_s$) | $1.68 \times 10^{-3}$ Ω·m |
| RF flux density ($B_1$) | $6.0 \times 10^{-5}$ T/A |
| Temperature ($T_C$) | 308 K |

The RF flux density $B_1$ was calculated using the Biot-Savart law given as

$$B_1 = \mu_0 \frac{r_C^2}{2\left(r_C^2 + d_C^2\right)^{3/2}} \tag{7}$$

where $\mu_0$ is permeability of free space, $r_C$ is the radius of the detector coil, and $d_C$ is the distance between the perfusion chamber and the detector coil.

## IV. Experimental Setup

In order to establish the hemoglobin-free condition with perfusing aCSF during acquisition of MRI data, we developed an MRI-compatible sample holder and perfusion system for a rat brain slice. We designed the experimental setup to use the same perfusion chamber in order to keep the interactions between the MRI acquisition data and the distribution of electric potential.

*A. MRI-compatible Sample Holder*

The non-magnetic material sample holder consisted of a perfusing chamber holder, a perfusing system for pumping aCSF in and out, and a detecting coil holder for MRI. It was made of polyvinyl chloride (PVC) so as not to contribute to the uniformity of the static magnetic field in MRI system. In order to position the detector coil closer to the source of the

magnetic field, a detecting coil holder was designed. A drain for the aCSF was prepared in case of perfusion failure around the chamber.

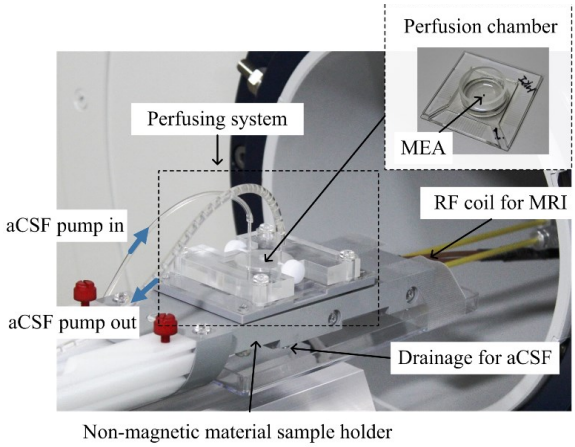


Figure 2. MRI-compatible non-magnetic sample holder and perfusing system

### *B. Multi-electrode Array and Perfusing system*

The construction of the perfusion chamber and perfusing system is shown in Fig. 3 (a). The perfusion chamber was a commercial chamber (Med Probe MED-P515A, Alpha Med Scientific, Inc.) that was fabricated for recording extra-cellular electric potentials in 64 channels by a commercial amplifier (MED-A64HE1 and MED-A64MD1, Alpha Med Scientific, Inc.). A multi-electrode array (MEA) of 8 × 8 channels was patterned on the bottom substrate for stimulation and measurement of extra-cellular electrical potential. The perfusion system consisted of tubes for pumping aCSF in and out and a gas channel for a mixture gas. In order to control the aCSF flow in the perfusion chamber, a space filler was designed and inserted. A sinker was placed on the rat brain slice to make contact with the bottom of the perfusion chamber and the MEA. Figure 3 (b) shows the relative positions of the space filler, the sinker, and the rat brain slice in the perfusion chamber.

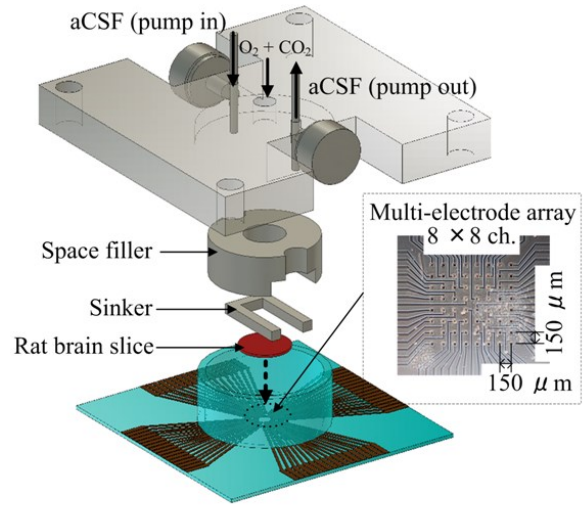


(a) Construction of perfusion chamber and perfusing system

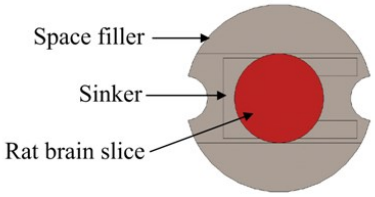


(b) Position relation in perfusion chamber

Figure 3. Structure of perfusing system and components in the perfusion chamber

## V. Results and Discussion

The magnetic field intensity on a rat brain slice was evaluated from the measured distribution of electric potential. A rat brain was extracted quickly under anesthesia with diethyl ether, and sliced with a thickness of 400μm. The sliced rat brain sample was physiologically recovered in room temperature for 1 hour. The brain slice was immersed in aCSF composed of 124 mM NaCl, 26 mM $NaHCO_3$, 10 mM glucose, 3 mM KCl, 1.25 mM $NaH_2PO_4$, 2 mM $CaCl_2$, and 2 mM $MgCl_2$ with supplying the mixture gas of $O_2$(95%) and $CO_2$(5%). Field excitatory postsynaptic potentials (fEPSPs) at an activating area in the brain slices were recorded in a 64-channel multi-electrode array with electrical stimulation of 22 μA. The calculated local magnetic field distributions at the activating area in the brain slices exhibited a maximum magnetic field intensity of $1.4 \times 10^{-11}$ T.

The theoretical and experimental sensitivities were evaluated with the same MRI acquisition parameters shown in Table III.

TABLE III. MRI ACQUISITION PARAMETERS

| | |
|---|---|
| Main static field ($B_0$) | 7 T |
| Repetition time ($T_R$) | 330 ms |
| Echo time ($T_E$) | 20 ms |
| Field of view ($L$) | 25 mm |
| Slice thickness ($h$) | 1 mm |
| Flip angle ($\theta$) | 30° |
| Number of voxels ($n$) | 40 |
| Receiver bandwidth ($\Delta f$) | 50 kHz |

The calculated theoretical sensitivity is given in Table IV. The signal intensity was $4.0 \times 10^{-4}$ V, and the noise intensity was $7.2 \times 10^{-7}$ V. These values resulted in a calculated SNR of 566. The theoretical limit of sensitivity becomes $3.3 \times 10^{-10}$ T.

TABLE IV. THEORETICALLY ESTIMATED SIGNAL AND NOISE

| | |
|---|---|
| Signal intensity ($S$) | $4.0 \times 10^{-4}$ V |
| Noise intensity ($N$) | $7.2 \times 10^{-7}$ V |
| Signal-to-noise ratio (SNR) | 566 |

According to Eq. (6), direct detection of neuronal activities is considered to be possible with only a one-time acquisition of MRI when the SNR is higher than 13376. This SNR value is not experimentally realistic. Therefore, data averaging is essential in experimental and clinical studies. A magnetic field of $1.4 \times 10^{-11}$ T is detectable with data averaging of 560 readings in our calculation model. When the stimulations are

applied at 3 Hz, the time for MRI data acquisition would be approximately 3.1 min.

The present calculation model did not include several experimental factors such as the flow of aCSF in the perfusion chamber. Thus, we carried out a practical evaluation using a 7-T MRI system (BioSpec 70/20 USR, Bruker Co.). Figure 4 shows the MR image acquired by the echo-planar imaging (EPI) method with the same MRI acquisition parameters as in the calculation model. The aCSF was supplied to the chamber during the measurement at a flow velocity of 2 mL/min. The experimental SNR in MR image was evaluated with $SNR = \mu_S/\sigma_N$, where $\mu_S$ is the mean signal intensity in a region of interest in the brain slice and $\sigma_N$ is the standard deviation of the background noise. Through a detailed tuning of acquisition parameters for eliminating artifacts and distortions in MRI, the SNR reached 470 in the current experimental condition. At this SNR value, the sensitivity of the magnetic field was $4.0 \times 10^{-10}$ T. When data averaging is performed with 810 readings, neuronal magnetic fields of $1.4 \times 10^{-11}$ T becomes detectable. The MRI acquisition time would then take 4.5 min with electric stimulation at 3 Hz.

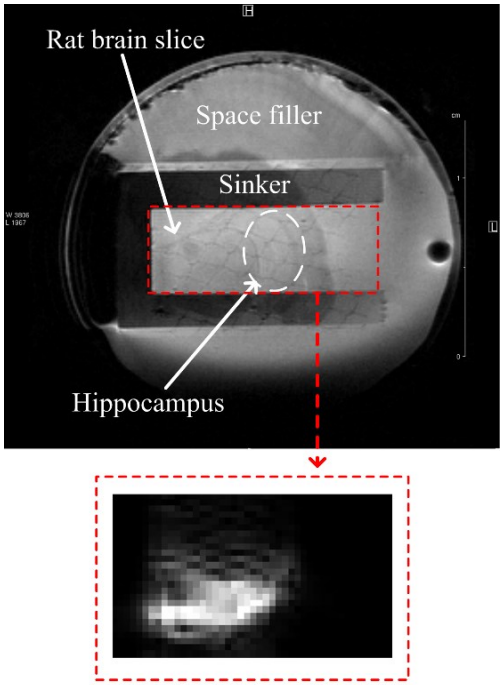


Figure 4. MR images of the rat brain slice placed in the perfusing chamber

Table V shows the comparison of the theoretical and experimental parameters for directly detecting a magnetic field of $1.4 \times 10^{-11}$ T resulting from the neuronal electric activities in rat brain slice. Furthermore, the results showed that the experimental SNR was very close to the theoretical value. This indicates that the developed experimental setup is feasible and the optimization process is sufficiently effective.

## VI. Conclusions

The theoretical sensitivity in MRI was evaluated based on an actual experimental setup for a rat brain slice maintained in a hemoglobin-free medium. The practical sensitivity was also evaluated in a 7-T MRI system with an MR image acquired by the EPI method. We achieved an experimental SNR value that was close to the theoretical result using the developed sample holder. These results demonstrated the feasibility of directly detecting neuronal electrical activities in a rat brain slice.

TABLE V. MRI ACQUISITION PARAMETERS FOR DIRECTLY DETECTING A MAGNETIC FIELD OF $1.4 \times 10^{-11}$ T

| | Theoretical evaluation | Practical evaluation |
|---|---|---|
| SNR | 566 | 470 |
| The number of averaged readings | 560 | 810 |
| MRI acquisition time at 3 Hz stimulation | 3.1 min. | 4.5 min. |

## References


[1] N. K. Logothetis, J. Pauls, M. Augath, T. Trinath, and A. Oeltermann, "Neurophysiological investigation of the basis of the fMRI signal", *Nature*, Vol. 412, pp.150–157, Jul. 2001.

[2] N. K. Logothetis, "What we can do and what we cannot do with fMRI", *Nature*, Vol. 453, pp.869–878, Jun. 2008.

[3] M. Joy , G. C. Scott and R. M. Henkelman , "In vivo detection of applied electric currents by magnetic resonance imaging", *Mag. Res. Imaging*, vol. 7, pp.89 -94, Jan. 1989

[4] J. Bodurka, A. Jesmanowicz, J.S. Hyde, H. Xu, L. Estkowski, S.J. Li, "Current-induced magnetic resonance phase imaging", *J. Magn. Reson.*, vol. 137, pp. 265–271, Mar. 1999

[5] J. Bodurka and P. A. Bandettini, "Toward direct mapping of neuronal activity: MRI detection of ultraweak, transient magnetic field changes", *Magn. Reson. Med.*, Vol. 47, No. 6, pp.1052–1058, Jun. 2002.

[6] H. Kamei, K. Iramina, K. Yoshikawa, and S. Ueno, "Neuronal current distribution imaging using magnetic resonance", *IEEE Trans. Magn.*, Vol. 35, No. 5-2, pp.4109–4111, Sep. 1999.

[7] J. Xiong, P. T. Fox, and J. H. Gao, "Directly mapping magnetic field effects of neuronal activity by magnetic resonance imaging", *Hum. Brain. Mapp*, Vol. 20, No. 41, pp.41–49, Sep. 2003.

[8] T. Hatada, M. Sekino, and S. Ueno, "Detection of weak magnetic fields induced by electrical currents using MRI: Theoretical and practical limits of sensitivity", *Magn. Reson. Med. Sci.*, Vol. 3, No. 4, pp.159–163, Jul. 2004.

[9] T. Hatada, M. Sekino, and S. Ueno, "FEM-based calculation of the theoretical limit of sensitivity for detecting weak magnetic fields in the human brain using magnetic resonance imaging", *J. Appl. Phys.*, Vol. 97, No. 10, pp.10E109–10E109-3, May 2005.

[10] T.-K. Truong, and A. W. Song, "Finding neuroelectric activity under magnetic-field oscillations (NAMO) with magnetic resonance imaging in vivo", *Proc. Natl. Acad. Sci. U. S. A.*, vol. 103, no. 33, pp.12598-12601, Aug. 2006

[11] Sekino M, Ohsaki H, Yamaguchi-Sekino S, Ueno S: "Toward Detection of Transient Changes in Magnetic-Resonance Signal Intensity Arising From Neuronal Electrical Activities", *IEEE Trans. Magn.*, Vol. 45, No. 10, pp.4841–4844, Oct. 2009.

[12] R. Chu, J.A. de Zwart, P. van Gelderen, M. Fukunaga, P. Kellman, T. Holroyd and J. H. Duyn, "Hunting for neuronal currents: absence of rapid MRI signal changes during visual-evoked response", *NeuroImage*, vol. 23, no. 3, pp. 1059–1067, Nov. 2004

[13] N. Petridou, D. Plenz, A. C. Silva, M. Loew, J. Bodurka, and P. A. Bandettini, "Direct magnetic resonance detection of neuronal electrical activity", *Proc. Natl. Acad. Sci. U. S. A.*, Vol. 103, No. 43, pp.16015–16020, Oct. 2006.

[14] T. S. Park, S. Y. Lee, J. Park, and S. Y. Lee, "Effect of nerve cell currents on MRI images in snail ganglia", *Neuroreport*, Vol. 15, No. 18, pp.2783–2786, Dec. 2004

[15] G. C. Scott, M. L. G. Joy, R. L. Armstrong, and R. M. Hankelman, "Sensitivity of magnetic resonance current density imaging", *J. Magn. Reson.*, Vol. 97, No. 2, pp.235–254, Apr. 1992.